# Evidence for a transition from diffusion-controlled to thermally controlled solidification in metallic alloys

K. Eckler, R. F. Cochrane,* D. M. Herlach, and B. Feuerbacher
*Institut für Raumsimulation, Deutsche Forschungsanstalt für Luft- und Raumfahrt, D-5000 Köln 90, Germany*

M. Jurisch
*Zentralinstitut für Festkörperphysik und Werkstofforschung, D-8027 Dresden, Germany*
(Received 21 June 1991)

Dendrite growth velocities have been measured as a function of undercooling in droplets of dilute alloys of B in Ni undercooled by up to 306 K using an electromagnetic levitation technique. At a critical undercooling, depending strongly on the B concentration, a steep rise of the dendrite growth velocity is observed. The analysis of the results within current theories of dendrite growth gives evidence for a transition from diffusion-limited to purely thermally controlled growth with partitionless solidification as a consequence.

Rapid solidification processing is a well-established method for the preparation of metastable materials, giving access to a range of materials properties, in particular supersaturated solid solutions. Here the crystal-growth velocity is the decisive parameter governing the trapping of solute in the solvent material.[1-5] Rapid solidification is usually achieved by rapidly quenching the melt in techniques such as melt spinning or atomization. However, such experiments do not allow direct investigations of the growth process. They are restricted to analyses of the already solidified products, which are subject to considerable modification of the material through, e.g., aging processes.

Alternatively, rapid solidification conditions prevail even at slow cooling rates of bulk melts, provided that a substantial amount of undercooling is achieved prior to solidification. The high driving force for crystallization accumulated in this way leads to rapid crystallization, which can be observed quantitatively. In the present case, an electromagnetic levitation technique has been used to avoid heterogeneous nucleation on container walls,[6] with the extra benefit of a suspended drop accessible to direct observation and even external stimulation of solidification.[7]

The dominant crystal-growth mechanism in undercooled melts is dendritic growth, which has attracted recent attention, both theoretical[8-10] and experimental.[11,12] In particular, measurements of the dendrite growth velocity as a function of undercooling on levitation undercooled Cu-Ni alloys[13] have revealed that nonequilibrium effects at the crystallization front play a decisive role in rapid solidification. The measurements indicated a velocity dependent partition coefficient as predicted by theory at high solidification velocities,[1,4,5] in agreement with laser heating investigations.[2,3]

In this work, we report measurements of dendrite growth velocities as a function of undercooling on levitation undercooled dilute alloys of Ni-B which, in contrast to previously investigated alloys, are characterized by a small equilibrium partition coefficient $k_E \ll 1$. Such a system exhibits an extremely high sensitivity of the partition coefficient on the growth velocity, therefore allowing a direct observation of a theoretically predicted transition[1,4,5] from diffusion-controlled dendrite growth to the thermally controlled regime. This is evidenced by the observation of a sudden rise in the growth velocity at a critical undercooling temperature $\Delta T^*$. Undercoolings above the critical undercooling lead to almost partitionless solidification. This is confirmed by the analysis of the boron distribution in as-solidified microstructures.

Ni-B alloys were prepared from constituents of purity better than 99.99%. The sample mass was typically 1 g, corresponding to a 6-mm diameter. The electromagnetic levitation technique was used to establish undercooling conditions by containerless processing in an ultrapure environment. The temperature of the sample was monitored in absolute terms by a two-color pyrometer with an accuracy of $\pm 3$ K at a sampling rate of 100 Hz. Solidification was initiated externally at a well-defined geometric position on the sample and at a preselected undercooling temperature. Measuring the time needed by the solidification front to sweep across the sample surface by imaging it onto a fast responding photodiode, allows one to determine the dendrite growth velocity quantitatively with an accuracy of better than 5%. Details about the levitation chamber and the measurements of solidification velocities in undercooled melts are given elsewhere.[7,14] Analysis of the boron distribution in the as-solidified samples were performed by neutron induced autoradiography.[15] This method is based on the $^{10}B(n,\alpha)^7Li$ reaction with the detection of $\alpha$ particles and $^7Li$ recoils using a solid-state nuclear track detector (SSNTD). Commercially available 0.1-mm-thick cellulose acetate foils in close contact to the specimen surface were used as a SSNTD. The samples were irradiated by thermal neutrons from a paraffin moderated $^{252}Cf$ source.

Figure 1 shows the measured growth velocity $V$ as a function of undercooling $\Delta T$ for pure Ni (open circles), Ni–0.7 at. % B (open squares) and Ni–1 at. % B (solid circles). For undercoolings less than a critical undercool-

 

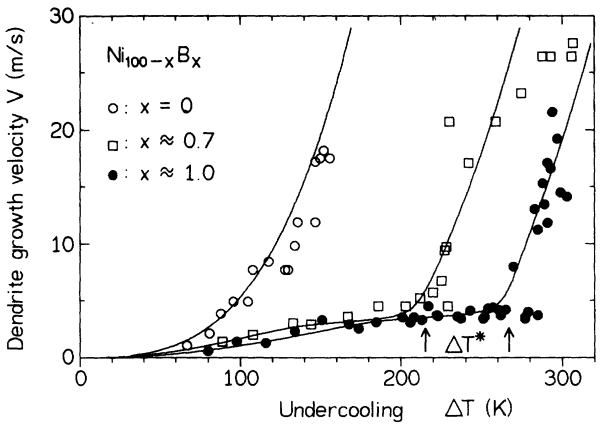


FIG. 1. Measured dendrite growth velocities $V$ as a function of undercooling $\Delta T$ for pure Ni (open circles); a dilute alloy of composition $Ni_{99.3}B_{0.7}$ (open squares) and an alloy of composition $Ni_{99}B_1$ (solid circles). The solid lines correspond to predictions according to the dendrite growth theory.

ing $\Delta T^*$, which depends on alloy concentration, the growth velocities of the alloys are much smaller than those of the pure metal. At the critical undercooling $\Delta T^* = 214$ K for $Ni_{99.3}B_{0.7}$ and $\Delta T^* = 267$ K for $Ni_{99}B_1$, respectively, the growth velocities sharply rise.

The interpretation of the results is based on the theoretical development by Boettinger, Coriell, and Trivedi,[10] which includes nonequilibrium effects in rapid dendrite growth. According to this model the total undercooling is expressed as a sum of different contributions:

$$\Delta T = \Delta T_t + \Delta T_r + \Delta T_c + \Delta T_k \ , \tag{1}$$

with the thermal undercooling $\Delta T_t$

$$\Delta T_t = \Delta T_{\rm hyp} P_t \exp(P_t) E_1(P_t) \equiv \Delta T_{\rm hyp} F_{\rm Iv}(P_T) \ , \tag{1a}$$

where the Ivantsov-function is defined as $F_{\rm Iv}(x) \equiv x \exp(x) E(x)$, the curvature undercooling $\Delta T_r$

$$\Delta T_r = 2\Gamma / R \ , \tag{1b}$$

the constitutional undercooling $\Delta T_c$

$$\Delta T_c = m c_0 \left[ 1 - \frac{m^*/m}{1-[1-k(V)]F_{\rm Iv}(P_c)} \right] , \tag{1c}$$

and the kinetic undercooling $\Delta T_k$

$$\Delta T_k = V/\mu \ . \tag{1d}$$

The symbols denote $\Delta T_{\rm hyp} = \Delta H_f / C_p^l$ the hypercooling limit, $P_t = VR/(2\alpha)$ the thermal Péclet number, $R$ the radius of the dendrite tip, $E_1$ the first exponential integral function, $F_{\rm Iv}$ the Ivantsov function, $\Gamma = \sigma / \Delta S_f$ the Gibbs-Thomson coefficient, $\Delta S_f$ the entropy of fusion, $c_0$ the nominal composition of the alloy, $k(V)$ the velocity dependent partition coefficient, $P_c = VR/(2D)$ the chemical Péclet number, and $\mu = (\Delta H_f V_0)/(k_B T_L^2)$ the interfacial kinetic coefficient according to the model of collision limited growth[16] with $k_B$ the Boltzmann constant. The other symbols are explained in Table I. The deviations from chemical equilibrium at the solidi-liquid interface are described by the velocity dependent partition coefficient $k(V)$[1] and the ratio of $m^*/m$,[10] defined as

$$k = k(V) = \frac{k_E + V/V_D}{1 + V/V_D} \tag{2a}$$

and

$$\frac{m^*}{m} = 1 + \frac{k_E - k(V)[1 - \ln(k(V)/k_e)]}{1 - k_E} \ , \tag{2b}$$

where $k_E$ is the equilibrium partition coefficient and $V_D = D/a_0$ is the atomic diffusive speed ($a_0$ interatomic spacing). Equation (1) in combination with Eq. (2) provides a relationship between the total undercooling $\Delta T$ and the product of $VR$ in terms of the Péclet numbers. Therefore, a second criterion is required in order to predict the growth velocity as a function of undercooling. Following Lipton, Kurz, and Trevidi[8] we use the marginal stability criterion,[17] which relates the dendrite tip radius to the marginally stable wavelength of perturbations at the solid-liquid interface. The resulting equation for the tip radius reads

$$R = \Gamma/\sigma^* \Big/ \left[ \Delta T_{\rm hyp} P_t \xi_t - \frac{2mc_0[1-k(V)]P_c}{1-[1-k(V)]F_{\rm Iv}(P_c)} \xi_c \right] , \tag{3}$$

where

$$\xi_t = 1 - \frac{1}{[1 + 1/(\sigma^* P_t^2)]^{1/2}} \tag{3a}$$

TABLE I. Material parameters of dilute Ni-B alloys as used in the calculations of dendrite growth.

| Parameter | | | Value |
|---|---|---|---|
| Heat of fusion | $\Delta H_f$ | (J/mol) | $1.72\times10^4$ |
| Specific heat of the liquid | $C_p^l$ | (J/mol K) | 36.39 |
| Liquidus slope | $m$ | K/at. % | −14.3 |
| Liquidus temperature (Ni) | $T_l$ | K | 1726 |
| Solid-liquid interface energy | $\sigma$ | J/m$^2$ | 0.464 |
| Diffusion coefficient of B in l-Ni | $D$ | m$^2$/s | $2.42\times10^{-9}$ |
| Thermal diffusivity of l-Ni | $\alpha$ | m$^2$/s | $1.0\times^{-5}$ |
| Equilibrium partition coefficient | $k_E$ | | $8.0\times10^{-6}$ |
| Speed of sound in l-Ni | $V_0$ | m/s | $2\times10^3$ |
| Diffusion velocity of B in l-Ni | $V_D$ | (m/s) | 7.6 |

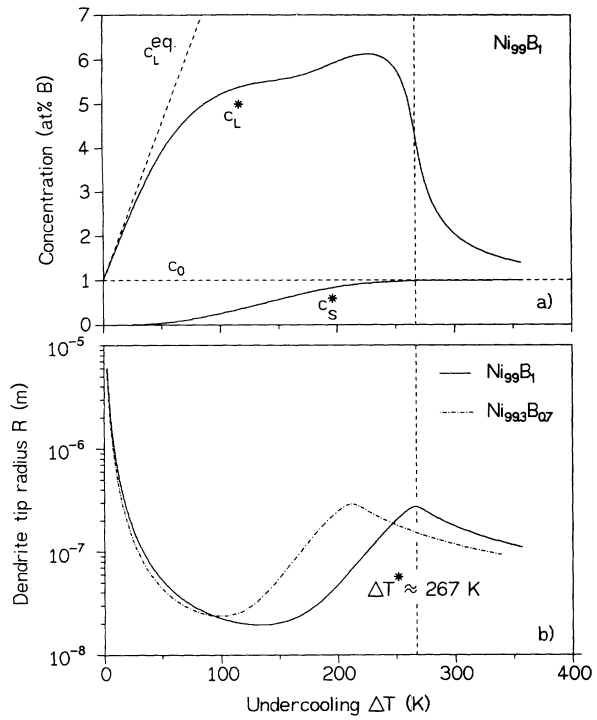


FIG. 2. (a) Calculated concentrations at the dendrite tip as a function of undercooling for the Ni–1 at. % B alloy. ($c_0$ nominal solute concentration, $c_L^*$ solute concentration of the liquid at the tip, $c_S^*$ solute concentration of the growing dendrite, and $c_L^{eq}$ equilibrium liquidus line.) (b) Calculated tip radius as a function of undercooling for the Ni–1 at. % B alloy (solid line) and the Ni-0.7 at. % B alloy (dashed line).

and

$$\xi_c = 1 + \frac{2k(V)}{1-2k(V)-[1+1/(\sigma^* P_c^2)]^{1/2}} \ . \tag{3b}$$

Here $\sigma^* = 1/(4\pi^2)$ denotes a stability constant. The procedure used was to specify a velocity $V$, solve Eq. (3) for $R$ numerically, and then evaluate $\Delta T$ according to Eq. (1). The results of these calculations for pure Ni, Ni–0.7 at. % B and Ni–1 at. % B, respectively, are given by the solid lines in Fig. 1. The data used for the calculations are taken from Table I. The data for pure Ni are free of adjustable parameters, while the alloy data have been fitted using an equilibrium partition coefficient of $k_E = 8 \times 10^{-6}$, as no reliable values were available from literature.

In order to investigate the conditions of solute trapping during rapid dendrite growth the concentrations at the dendrite tip in the liquid $c_L^*$ and in the solid $c_s^*$, respectively, are calculated according to[10]

$$c_L^* = \frac{c_0}{1-[1-k(V)]F_{\mathrm{Iv}}(P_c)} \ , \tag{4a}$$

$$c_S^* = k(V) c_L^* \ . \tag{4b}$$

The results of such calculations are plotted versus the undercooling for the Ni-1 at. % B sample in Fig. 2(a). The boron concentration in the liquid at the interface $c_L^*$ initially grows rapidly with undercooling due to solute rejection, but levels off as nonequilibrium processes become important. The sharp increase of the growth velocities sets in at a solute concentration $c_S^*$ of the growing crystal very close to the nominal concentration of the melt, due to the solute trapping effects. Figure 2(a) suggests that at undercoolings beyond $\Delta T = 267$ K solidification should be almost partitionless.

The critical undercooling is more pronounced in the calculated tip radius as a function of undercooling as shown in Fig. 2(b) for both alloys. At low undercoolings the tip radius decreases due to the increase of the thermal and solutal gradients ahead of the solidification front. As the undercooling is increased, the radius of the dendrite tip rises, owing to the fact that the growth velocities approach the velocity of absolute stability for solutal dendrites, paralleled by a decrease of the solutal gradient caused by the velocity dependent partition coefficient. Beyond the critical undercooling the growth is now purely thermally controlled, indicated by the observation that the tip radius begins to fall again. In this regime dendrite growth takes place nearly without segregation, resulting

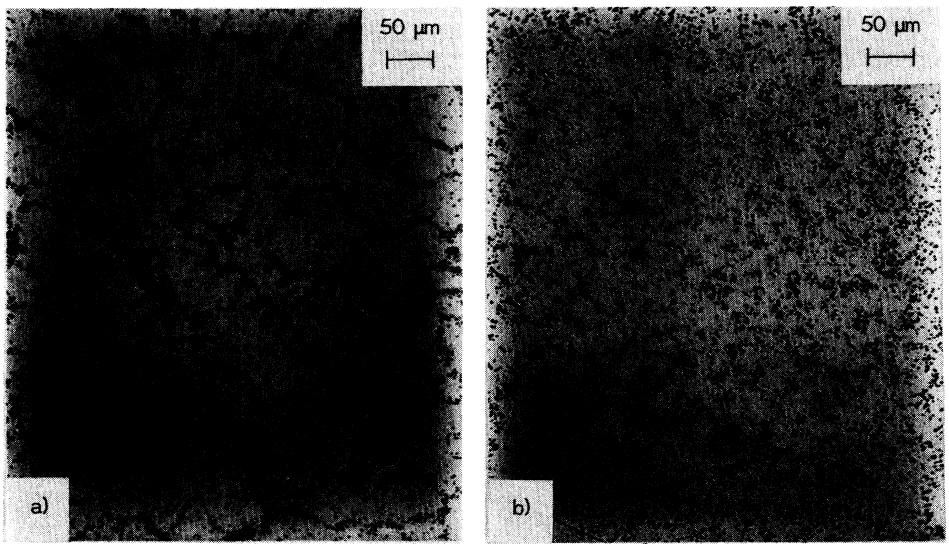


FIG. 3. Boron distribution across the sample as determined by SSNTD for an $Ni_{99.3}B_{0.7}$ alloy; dark regions: boron rich, light regions: boron poor, left side (a) a sample undercooled by $\Delta T = 60$ K $< \Delta T^*$, right side (b) a sample undercooled by $\Delta T = 306$ K $> \Delta T^*$.

in a highly supersaturated crystal.

The predictions of solute trapping and partitionless solidification from the analysis of the dendrite growth behavior are confirmed qualitatively by the autoradiograms given in Fig. 3 for two samples of $Ni_{99.3}B_{0.7}$ undercooled by 60 K (a) and 306 K (b), respectively. The dark regions characterized by an increased etchpit density correspond to boron rich phase, whereas the light regions give the boron poor regions. In the microstructure of the sample undercooled moderately by 60 K boron is segregated *into the grain boundaries* and/or partly precipitated into a boron rich phase (probably $Ni_3B$) within the interdendritic spaces. Inside the interdendritic regions, the boron concentration was below the detection limit of the method. On the other hand, the sample undercooled by the maximum amount of 306 K reveals an almost homogeneous distribution of B across the sample with an enhanced, easily detectable B concentration *inside the grains,* representing the supersaturated state of this alloy. Note this is true despite the fact that the dendrite tip radius in the sample undercooled by 60 K is *smaller* than that in the sample undercooled by 306 K [cf. Fig. 2(b)]. It should be carried in mind that the boron rich precipitates found in this largely undercooled sample probably indicate secondary reactions of precipitation during the cooling of the solidified sample.

In summary, the dendrite growth velocities measured as a function of undercooling on levitation undercooled dilute Ni-B alloys are well described within the current theory of dendrite growth taking into account deviations from local equilibrium at the solid-liquid interface. Owing to the small equilibrium partition coefficient of the Ni-B system, the solute trapping effect is very pronounced, resulting in a steep rise of the growth velocities at a critical undercooling $\Delta T^*$. The value of $\Delta T^*$ depends sensitively on the alloy composition. At undercoolings less than $\Delta T^*$, growth is governed by both redistribution of heat and solute, whereas at undercoolings larger than $\Delta T^*$ growth is purely thermally controlled with the consequence of partitionless solidification at the largest undercoolings. This has been confirmed by investigations of the boron distribution in as-solidified samples undercooled by different amounts by the SSNTD method. The present investigations are of fundamental interest in the understanding of the development of supersaturated alloys and the clarification of the processing conditions for their reproducible preparation.

The authors thank W. Löser for helpful discussions, H. Grill and H. Mühlmeyer for technical assistance.

---

*Present address: University of Leeds, School of Materials, Leeds LS2 9JT, United Kingdom.

[1]M. J. Aziz, J. Appl. Phys. **53**, 1158 (1982).

[2]M. Aziz, J. Y. Tsao, M. O. Thompson, P. S. Peercy, and C. W. White, Phys. Rev. Lett. **56**, 2489 (1986).

[3]M. J. Aziz and C. W. White, Phys. Rev. Lett. **57**, 2675 (1986).

[4]W. J. Boettinger and M. J. Aziz, Acta Metall. **37**, 3379 (1989).

[5]W. J. Boettinger, S. R. Coriell, and R. F. Sekerka, Mater. Sci. Eng. **65**, 27 (1984).

[6]R. Willnecker, D. M. Herlach, and B. Feuerbacher, Appl. Phys. Lett. **49**, 1339 (1986).

[7]E. Schleip, R. Willnecker, D. M. Herlach, and G. P. Görler, Mater. Sci. Eng. **98**, 39 (1988).

[8]J. Lipton, W. Kurz, and R. Trivedi, Acta Metall. **35**, 957 (1987); **35**, 965 (1987).

[9]Y. Saito, C. Misbah, and H. Müller-Krumbhaar, Phys. Rev. Lett. **63**, 2377 (1989).

[10]W. J. Boettinger, S. R. Coriell, and R. Trivedi, in *Rapid Solidification Processing-Principles and Technologies IV,* edited by R. Mehrabian and P. A. Parrish (Claitor's, Baton Rouge, 1988), p. 13.

[11]H. Chou and H. Z. Cummins, Phys. Rev. Lett. **61**, 173 (1988).

[12]T. J. Piccone, Y. Wu, Y. Shiohara, and M. Flemings, Metall. Trans. A **18**, 915 (1987); **18**, 925 (1987).

[13]R. Willnecker, D. M. Herlach, and B. Feuerbacher, Phys. Rev. Lett. **62**, 2709 (1989).

[14]D. M. Herlach, R. Willnecker, and F. Gillessen, in *5th European Symposium on Material Sciences under Microgravity–Results of SPACELAB-1,* edited by T. D. Guyenne (European Space Agency, Scientific and Technical Publications Branch, Noordwijk, 1984), p. 399.

[15]J. D. H. Hughef and G. T. Rogers, J. Instrum. Met. **95**, 299 (1967).

[16]D. Turnbull, Metall. Trans. A **12**, 693 (1981).

[17]J. S. Langer and H. Müller-Krumbhaar, Acta Metall. **26**, 1689 (1978); **26**, 1697 (1978).

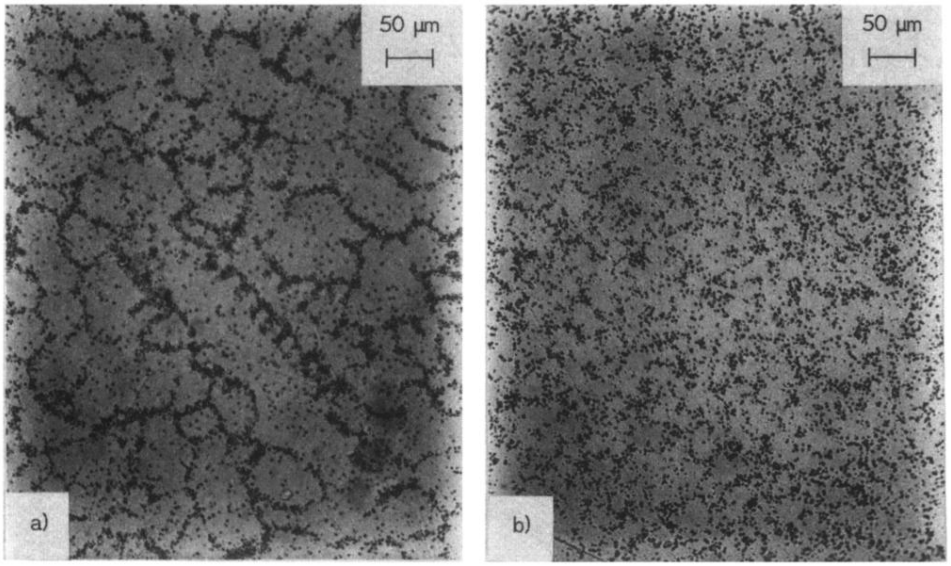


FIG. 3. Boron distribution across the sample as determined by SSNTD for an $Ni_{99.3}B_{0.7}$ alloy; dark regions: boron rich, light regions: boron poor, left side (a) a sample undercooled by $\Delta T = 60\ \mathrm{K} < \Delta T^*$, right side (b) a sample undercooled by $\Delta T = 306\ \mathrm{K} > \Delta T^*$.